The Institution of Engineers, Australia
8th National Conference on Hydraulics in Water Engineering
ANA Hotel Gold Coast, Australia 13-16 July 2004

Scale Effects in Moderate Slope Stepped Spillways Experimental Studies in Air-Water Flows

C.A. Gonzalez
B.E., M.E.
Ph.D. student, Dept of Civil Engineering, The University of Queensland, Brisbane 4072, Australia
H. Chanson
M.E., ENSHMG, INSTN, Ph.D., DEng., Eur.Ing., IEAust., IAHR
Reader, Dept of Civil Engineering, The University of Queensland, Brisbane 4072, Australia

Abstract: Air-water flow measurements were conducted in two large-size stepped chute facilities (θ = 3.4 & 16º) to study experimental distortion caused by scale effects and result extrapolation to prototypes. The stepped geometries corresponded to moderate slopes typical of embankment dams and storm waterways. Experimental data included distributions of air concentration, air-water flow velocity, bubble frequency, bubble chord length and turbulence intensity. For a Froude similitude, scale effects were observed in both facilities, although the geometric scaling ratio was only $L_r = 2$ in each case. The criterion selection for scale effects is a critical issue. In the 16º chute, major differences (i.e. scale effects) were observed in terms of bubble chord sizes and turbulence levels although little scale effects were seen in terms of void fraction and velocity distributions. The findings emphasise that physical modelling of stepped chutes based upon a Froude similitude is more sensitive to scale effects than classical smooth-invert chute studies. This is consistent with basic dimensional analysis.

Keywords: physical modelling, scale effects, stepped spillways, air entrainment, embankment dams.

1. INTRODUCTION

During the last three decades, research in the hydraulics of stepped spillways has been very active (Chanson 2001, Ohtsu and Yasuda 1998). For a given stepped chute, water flows as a succession of free-falling nappes (nappe flow regime) at small discharges. For an intermediate range of flow rates, a transition flow regime is observed. Most prototype spillways operate at large discharges per unit width (i.e. skimming flow regime) for which the waters skim as a coherent stream over the pseudo-bottom formed by step edges (Fig. 1 & 2). Skimming flows are characterised by very-significant form losses and momentum transfer from the main stream to the recirculation zones. There is an obvious analogy with skimming flows past large elements and boundary layer flows past d-type roughness: e.g., Knight and Macdonald (1979), Djenidi et al. (1999).Stepped chute hydraulics is not simple, because of different flow regimes, but most importantly because of strong flow aeration, very-strong turbulence, and interactions between entrained air and turbulence (Chanson and Toombes 2002). To date, little research was conducted at the microscopic scale on the complex nature of the flow and its physical modelling.

It is the purpose of this study to discuss similitude and scale effects affecting stepped chute flows. The analysis is supported by a series of systematic measurements conducted in two large-size facilities (θ = 3.4 and 16º) with two step sizes each. The geometric scaling ratio was $L_r = 2$ in each case. The results provide a new understanding of scale effects affecting stepped chute flows.

2. DIMENSIONAL ANALYSIS AND SIMILITUDE

2.1 Basic analysis

A dominant characteristic of stepped chute flows is the strong flow aeration ('white waters') clearly seen in prototype and laboratory (Fig. 1). Hence the relevant parameters needed for any dimensional analysis include the fluid properties and physical constants, the channel geometry and inflow conditions, the air-water flow properties including the entrained air bubble characteristics, and the geometry of the steps. Considering a skimming flow down a stepped chute with flat horizontal steps at uniform equilibrium and for a prismatic rectangular channel, a complete dimensional analysis yields a relationship between the local air-water flow properties, the fluid properties and physical constants, flow conditions, and step geometry :

$$C, \frac{V}{\sqrt{g*d}}, \frac{u'}{V}, \frac{d_{ab}}{d}, \ldots = F_1\left(\frac{x}{d}; \frac{y}{d}; \frac{q_w}{\sqrt{g*d^3}}; \rho_w * \frac{q_w}{\mu_w}; \frac{g*\mu_w^4}{\rho_w * \sigma^3}; \frac{d}{h}; \frac{W}{h}; \theta; \frac{k_s'}{h}\right) \quad (1)$$

where C is the local void fraction, V is the local velocity, g is the gravity acceleration, d is the equivalent water depth at uniform equilibrium, u' is a characteristic turbulent velocity, d_{ab} is a characteristic size of entrained bubble, x is the coordinate in the flow direction measured from a step edge, y is the distance normal from the pseudo-bottom formed by the step edges, q_w is the water discharge per unit width, ρ_w and μ_w are the water density and dynamic viscosity respectively, σ is the surface tension between air and water, W is the chute width, h is the step height, θ is the angle between the pseudo-bottom and the horizontal, and k_s' the skin roughness height (Fig. 2). For air-water flows, the equivalent clear water depth is defined as :

Fig. 1 - Skimming flow down Santa Cruz dam spillway at low overflow (Courtesy of US Bureau of Reclamation) - The 23-m wide stepped spillway is designed to accommodate the 25-year flood (57 m^3/s peak), wit larger floods passing over the dam crest - Note the splitter piers to aerate the undernappe (dam height: 46 m)

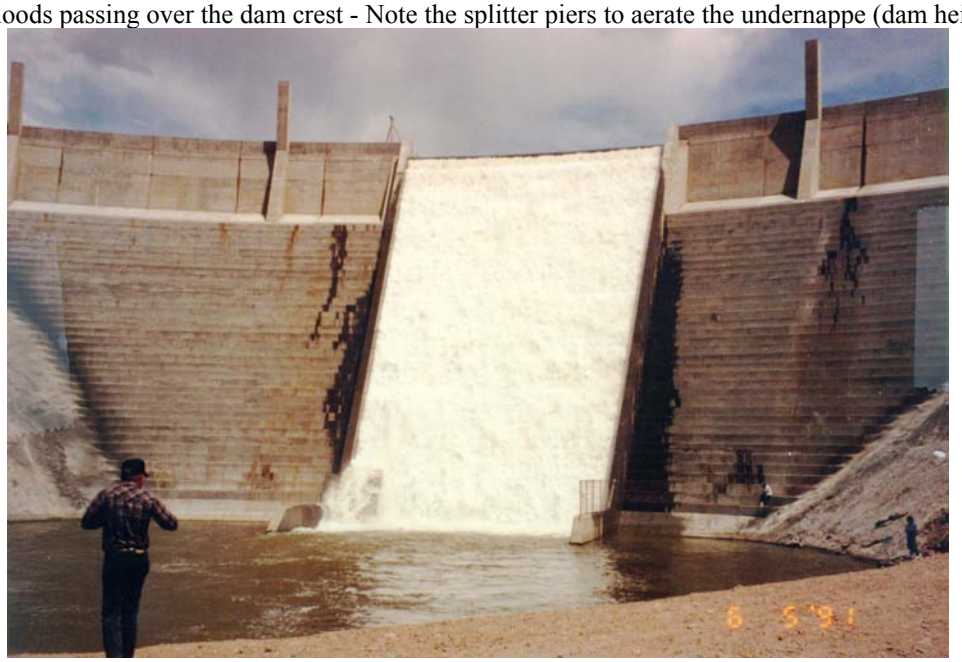

Fig. 2 - Skimming flow over a stepped chute : definition sketch

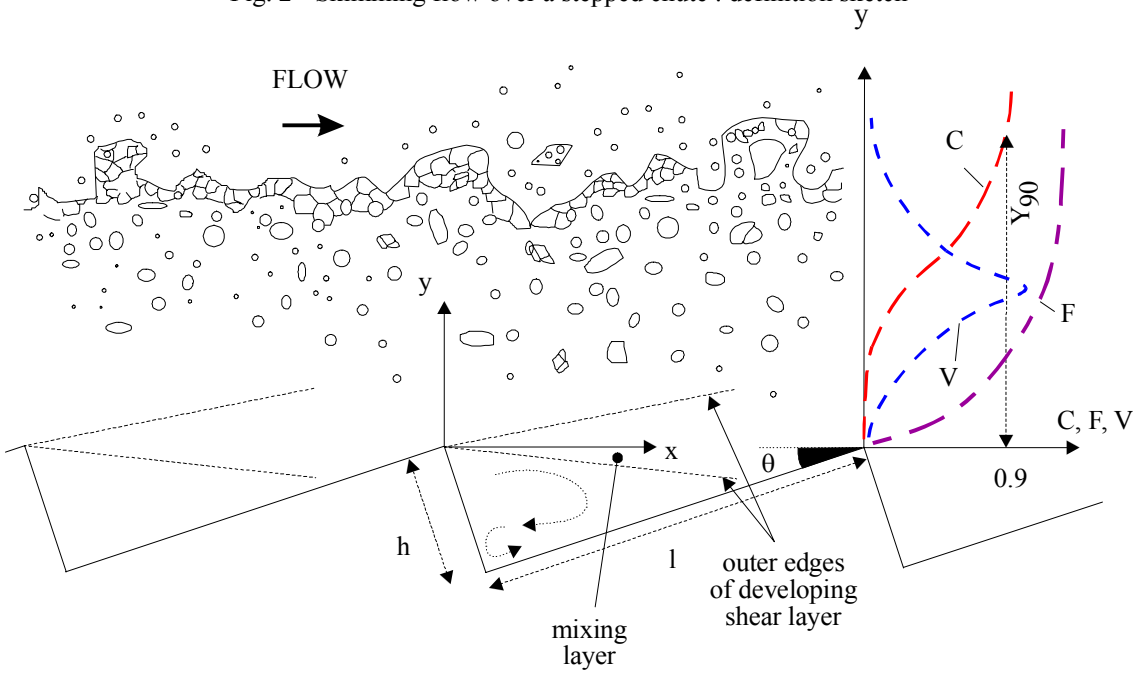

$$d = \int_{y=0}^{y=Y_{90}} (1 - C) * dy \quad (2)$$

where Y_{90} is the depth where C = 0.9. In Equation (1) right handside, the 3rd, 4th and 5th dimensionless terms are Froude, Reynolds and Morton numbers respectively, and the last four terms characterise the step cavity shape and the skin friction effects on the cavity wall. Note that any combination of dimensionless numbers is also dimensionless. One parameter among the Froude, Reynolds and Weber numbers can be replaced by the Morton number $Mo = (g*\mu_w^4)/(\rho_w*\sigma^3)$ as seen in Equation (1) where the Weber number was replaced. Further simplifications may be derived by considering the depth-averaged air-water flow properties. For a skimming flow at uniform equilibrium, Equations (1) yields :

$$F_2\left(\frac{U_w}{\sqrt{g * d}}; \rho_w \frac{U_w * d}{\mu_w}; \frac{g * \mu_w^4}{\rho_w * \sigma^3}; C_{mean}; \frac{d}{h}; \frac{W}{h}; \theta; \frac{k_s'}{h}\right) = 0 \quad (3)$$

where U_W is the mean flow velocity ($U_W = q_W/d$) and C_{mean} is the depth-averaged void fraction:

$$C_{mean} = \frac{1}{Y_{90}} * \int_{y=0}^{y=Y_{90}} C * dy \quad (4)$$

Despite very simplistic assumptions, Equation (1), and even Equation (3), demonstrate that dynamic similarity of stepped chute flows is impossible with geometrically similar models, unless working at full-scale, because of the large number of relevant parameters. In free-surface flows, most laboratory studies are based upon a Froude similitude (e.g. Henderson 1966, Chanson 2004). But cavity recirculation and momentum exchanges between cavity and stream flow are dominated by viscous effects suggesting the need for a Reynolds similitude. If L_r is the geometric scaling ratio defined as the ratio of prototype to model dimensions, it is impossible to satisfy simultaneously Froude and Reynolds similarities unless $L_r = 1$, and significant scale effects are expected on small size models ($L_r >> 1$). Usually the same fluids (air and water) are used in model and prototype, and the Morton number becomes an invariant.

Table 1. Summary of systematic studies on stepped chutes based upon a Froude similitude

Study (1)	Definition of scale effects (2)	Limiting conditions to avoid scale effects (3)	Experimental flow conditions (4)
BaCaRa (1991)	Flow resistance & energy dissipation	$L_r < 25$	Model studies: θ = 53.1º, h = 0.06, 0.028, 0.024, 0.014 m L_r = 10, 21.3, 25, 42.7
Boes (2000)	Void fraction & velocity distributions	Re > 1E+5	Model studies: θ = 30 & 50º, W = 0.5 m, h = 0.023 to 0.093 m L_r = 6.6, 13, 26 (30º) / 6.5, 20 (50º)
Chanson et al. (2002)	Flow resistance	Re > 1E+5 h > 0.02 m	Prototype & model studies θ = 5 to 50º, W = 0.2 to 15 m, h = 0.005 to 0.3 m, 3E+4 < Re < 2E+8, 32 < We < 6.5 E+6
Present study	Void fraction & bubble count rate distributions	$L_r < 2$	θ = 3.4º, W = 0.5 m, h = 0.143, 0.0715 m, 2.4 E+5 < Re < 6 E+5 L_r = 1, 2
	Void fraction, bubble count rate, velocity & turbulence level distributions, Bubble sizes & clustering	$L_r < 2$	θ = 16º, W = 1 m, h = 0.10, 0.05 m, 1.2E+5 < Re < 1.2 E+6 L_r = 1, 2

Notes : D_H : hydraulic diameter; L_r : geometric scaling ratio; $Re = V*D_H/\nu_W$; $We = \rho_W*V^2*d/\sigma$.

2.2 Discussion

Few studies tested systematically the validity of a Froude similitude with geometric similarity using same fluids in model and prototype (Table 1). BaCaRa (1991) described a systematic laboratory investigation of the M'Bali

dam spillway with model scales of L_r = 10, 21.3, 25 and 42.7. For the smallest models (L_r = 25 & 42.7), the flow resistance was improperly reproduced. Chanson et al. (2002) re-analysed more than 38 model studies and 4 prototype investigations with channel slopes ranging from 5.7º up to 55º, with Reynolds numbers between 3 E+4 and 2 E+8. They concluded that physical modelling of flow resistance may be conducted based upon a Froude similitude if laboratory flow conditions satisfy h > 0.020 m and Re > 1E+5. They added that true similarity of air entrainment was achieved only for model scales L_r < 10. However detailed studies of local air-water flow properties yielded more stringent conditions suggesting the impossibility to achieve dynamic similarity, even in large-size models (Table 1). In the present study, a Froude similitude was used as for most open channel flow studies and past studies.

3. EXPERIMENTAL SETUP

Experiments were performed in two facilities with flat horizontal steps (Table 2). The first channel was 24 m long 0.5 m wide with a 3.4º slope. Two step sizes were used : h = 0.143 and 0.0715 m. In both cases, the first drop was located 2.4 m downstream of a smooth nozzle (d_n = 0.03 m), and the channel invert, upstream of the vertical drop, was flat and horizontal for all experiments. Water was supplied by a pump, with a variable-speed electronic controller (Taian™ T-verter K1-420-M3 adjustable frequency AC motor drive), enabling an accurate discharge adjustment in a closed-circuit system. The flow rates were measured with a Dall™ tube flowmeter, calibrated on site. The accuracy of the discharge measurement was approximately 2%. The second channel was 1 m wide with a 15.9º slope. It consisted of a broad-crest followed by nine identical steps (h = 0.1 and 0.05 m). The flow rate was delivered by a pump controlled with an adjustable frequency AC motor drive, enabling an accurate discharge adjustment in a closed-circuit system. The discharge was measured from the upstream head above crest with an accuracy of about 2%, after complete calibration on the crest profile site.

Air-water flow properties were measured using a single-tip resistivity probe (∅ = 0.35 mm) in Channel 1 and a double-tip probe (∅ = 0.025 mm) in Channel 2. Both probes were developed at the University of Queensland and excited by an air bubble detector (AS25240). The probe signal was scanned at 5 kHz for 60 to 180 s in Channel 1, and at 20 kHz per sensor for 20 s in Channel 2. The probe signal outputs were post-processed using the method outlined by Chanson (2002) and Chanson and Toombes (2002). The translation of the probes in the direction normal to the channel invert was controlled by a fine adjustment travelling mechanism connected to a MitutoyoTM digimatic scale unit (Ref. No. 572-503). The error on the vertical position of the probe was less than 0.025 mm. Flow visualisations were conducted with a digital video-camera and high-speed still photographs.

Table 2. Summary of experimental flow conditions

Reference	θ deg.	q_W m^2/s	h m	d_c/h	Flow regime	Instrumentation	Remarks
(1)	(2)	(3)	(4)	(5)	(6)	(7)	(8)
Channel 1	3.4	0.150	0.143	0.92	Transition flow	Single-tip conductivity probe (∅ = 0.35 mm).	L = 24 m. W = 0.5 m. Inflow: pressurised intake. Experiment CR98.
		0.06	0.0715	1.0			Experiment EV200.
		0.08		1.2			
Channel 2	15.9	0.075 to 0.220	0.10	0.85 to 1.7	Transition & Skimming flows	Double-tip conductivity probe (∅ = 0.025 mm).	L = 4.2 m. W = 1 m. Inflow: uncontrolled broad-crest.
		0.020 to 0.08	0.05				

Notes : L : chute length; W : chute width.

4. EXPERIMENTAL RESULTS

4.1 Basic results

Detailed measurements of void fraction and air-water flow properties were conducted for a number of dimensionless flow rates d_c/h. Identical experiments were repeated with two step sizes in each Channel based upon a Froude similitude (Table 2). Systematic comparisons were performed. Overall the results showed that the distributions of air concentration were properly scaled with a Froude similitude, for the investigated flow conditions (Table 2). This is illustrated in Figures 3 and 4A for Channel 1 and 2 respectively, showing

dimensionless distributions of void fraction C. In addition, the void fraction distributions are compared with an analytical solution of the advection diffusion equation for air bubbles (Chanson and Toombes 2002).

Good agreement was observed also in terms of dimensionless distributions of velocity, as well as in terms of mean air content C_{mean}, dimensionless flow velocity U_w/V_c and air-water flow velocity V_{90}/V_c, where V_{90} is the air-water flow velocity at $y = Y_{90}$ and Y_{90} is the characteristic depth where C = 0.90 (Fig. 3 and 4A). However significant differences, hence scale effects, were observed in terms of dimensionless distributions of bubble count rates F^*d_c/V_c and of turbulence intensity Tu as functions of y/d_c where F is the bubble count rate defined as the number of bubbles impacting the probe per second, and d_c and V_c are the critical flow depth and velocity respectively. In both Channels 1 and 2, lesser dimensionless bubble count rates by about 30 to 50% were observed with the smallest step heights : i.e., h = 0.0715 and 0.05 m for θ = 3.4 and 15.9º respectively. This is illustrated in Figures 3 and 4B, and the finding implies significant scale effects in terms of number of entrained bubbles and bubble sizes. In Channel 2, differences in turbulence intensity distributions were consistently observed, with lesser maximum turbulence levels for the smallest step height (h = 0.05 m). This is well illustrated in Figure 4B. Further, in Channel 2, a comparative analysis of bubble chord size distributions, for similar flow rate, identical location and local void fraction, showed consistently differences between the two step heights : entrained bubbles were comparatively larger for the smallest model (Fig. 5A). Figure 5 compares dimensionless bubble and droplet chord sizes ch/d_c recorded at the same dimensionless distance from the inception point and for the same dimensionless flow rate with two step heights (h = 0.1 and 0.05 m). Figure 5A shows dimensionless bubble chord distributions for C = 0.1. Figure 5B presents dimensionless droplet chord distributions for C = 0.96, at the same locations as in Figure 5A for the two step heights. Basically entrained bubble sizes were not scaled at 2:1 (Fig. 5A). A similar observations was made in terms of water droplet size distributions in the spray region (Fig. 5B). In dimensional terms, the size distributions of the smallest bubbles and droplets were about the same for both step heights, but a broader range of large particles were seen with the largest step height (h = 0.1 m).

Overall the results demonstrated significant scale effects in terms of bubble and droplet size distributions that were not approximated properly by a Froude similitude.

Fig. 3 - Comparison of dimensionless distributions of void fraction C and bubble count rate F^*d_c/V_c in Channel 1 (θ = 3.4º, $d_c/h \sim 1$) for h = 0.143 and 0.0715 m - Step 9, x/l = 1 (step brink)

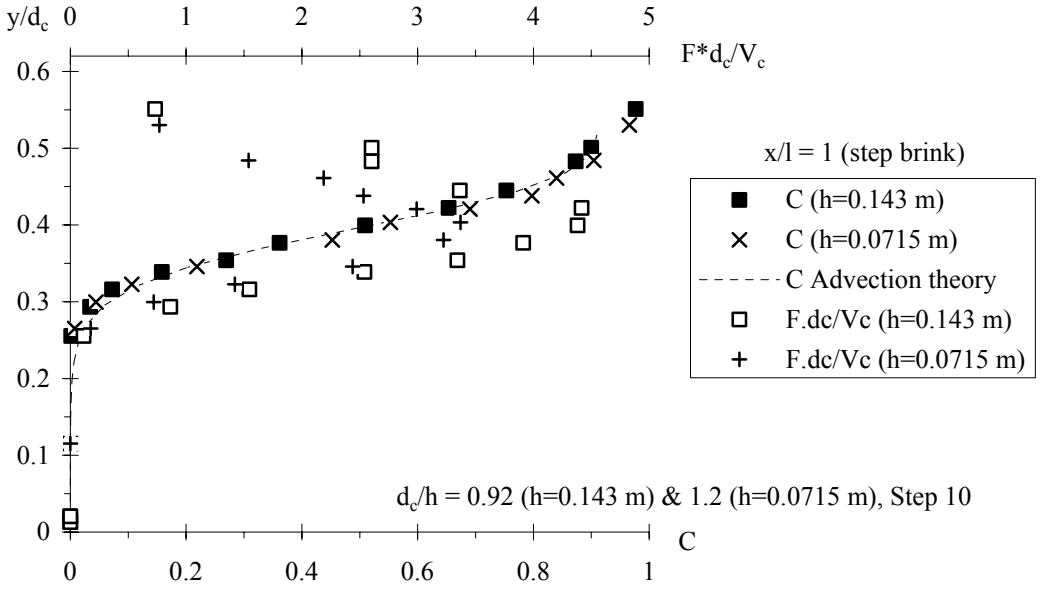

4.2 Discussion

A basic result is the lesser number of entrained bubbles and comparatively greater bubble sizes observed in the smallest flumes, as well as lower turbulence levels. The findings have direct implications on the flow structure and the interactions between turbulence and entrained bubbles. Chanson and Toombes (2002) demonstrated that the air-water flow turbulence level was a function of bubble count rate : $Tu \propto F^{1.5}$. Lesser turbulence levels in small laboratory flumes must imply lesser rate of energy dissipation, particularly on long chutes. That is, small-

size models are likely to underestimate the rate of energy dissipation of prototype stepped spillways for similar flow conditions. Similarly, the lesser number of entrained bubble sizes in laboratory flumes must affect the rate of air-water mass transfer on the chute. Present results imply that the air-water interface area, hence the rate of air-water mass transfer, are underestimated in small-size physical-models, and extrapolation are not reliable.

Fig. 4 - Comparison of dimensionless distributions of void fraction C, bubble count rate F^*d_c/V_c, velocity V/V_c and turbulence intensity Tu in Channel 2 (θ = 15.9°, d_c/h = 1.5) for h = 0.10 and 0.05 m at 3 step edges downstream of the inception of free-surface aeration

(A) Dimensionless distributions of void fraction C and velocity V/V_c

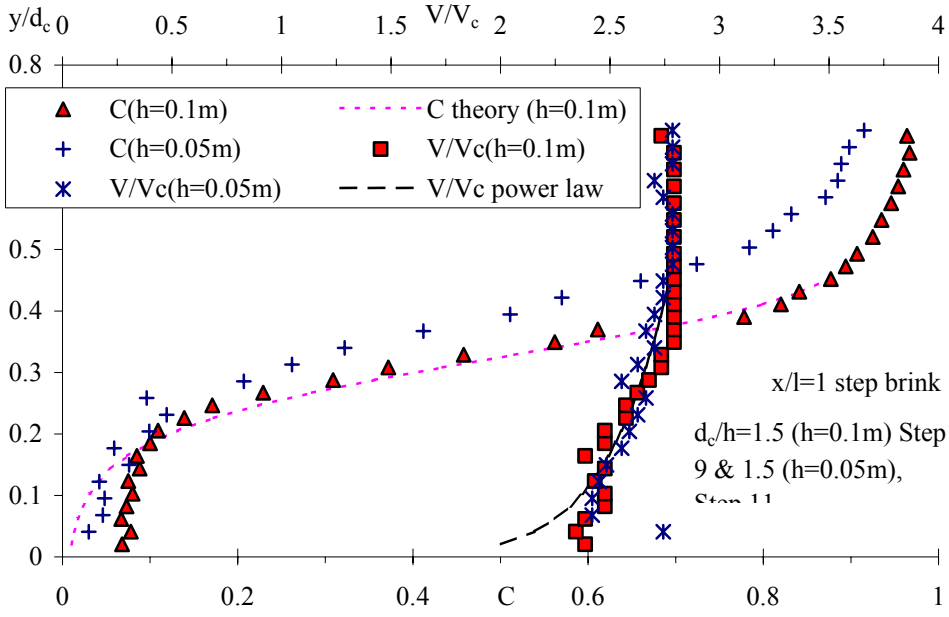

(B) Dimensionless distributions of bubble count rate F^*d_c/V_c and turbulence intensity Tu

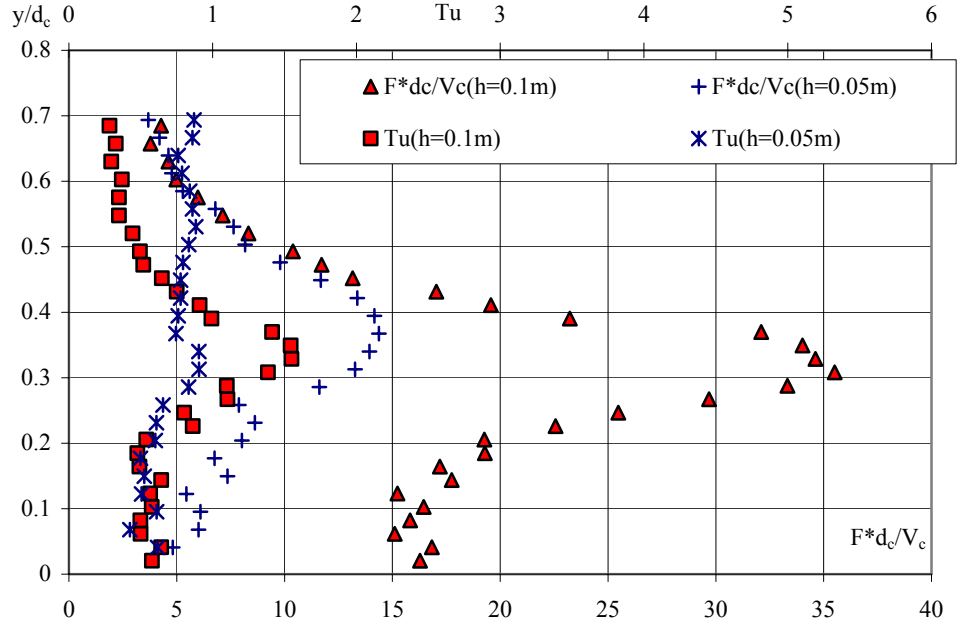

Fig. 5 - Comparison of dimensionless bubble and droplet chord size ch/d_c distributions in Channel 2 (θ = 15.9º, d_c/h = 1.5) for h = 0.10 and 0.05 m at step edges 9 and 14 respectively
(A) Bubble chord size distributions for C = 0.1

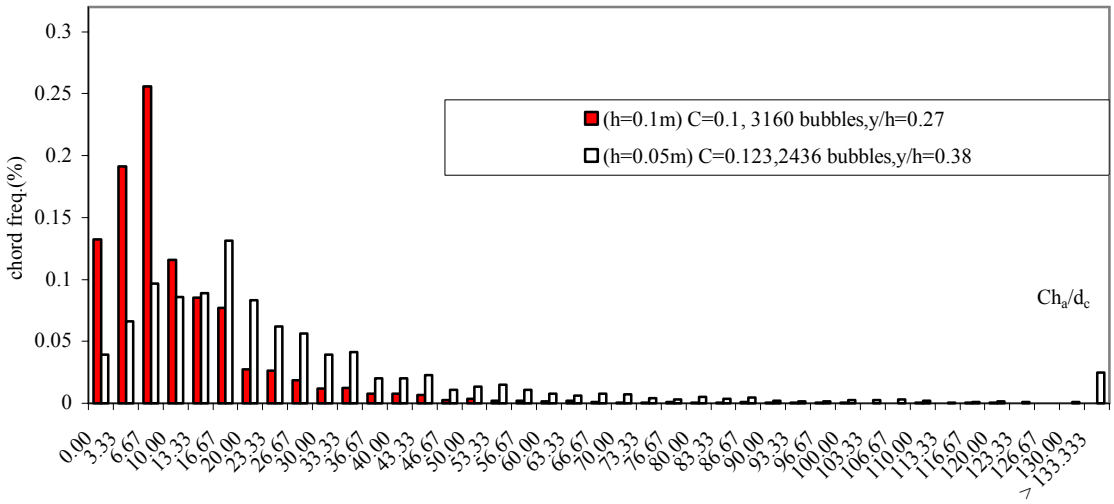

(B) Droplet chord size distributions for C = 0.96

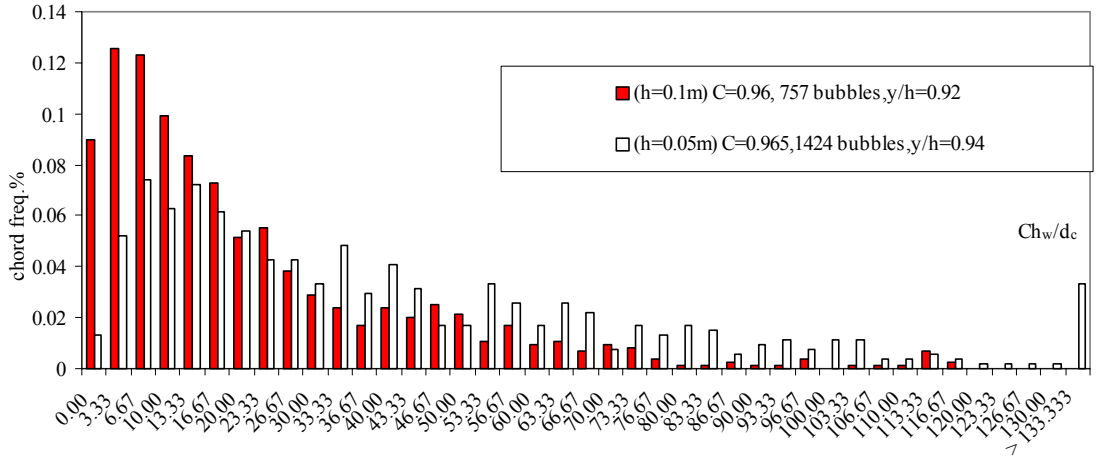

5. SUMMARY AND CONCLUSION

The study of stepped chute hydraulics is still based primarily upon physical modelling. It is understood that stepped chute hydraulics is complex because of different flow regimes, strong flow aeration, and interactions between entrained air and turbulence. A complete dimensional analysis yields two basic equations (1) and (3) corresponding respectively to two-dimensional and one-dimensional air-water flows. The analysis emphasises the complexity of stepped chute hydrodynamics, and the limitations of the Froude similitude. Systematic studies of scale effects affecting stepped chute flows are few and the results are sometimes contradictory.

New experimental works were conducted with two slopes (θ = 3.4 & 16º) and two large step sizes for each large-size facility. Identical experiments were performed based upon a Froude similitude with geometrically similar channel configurations. A geometric scaling ratio L_r = 2 was selected for both invert slopes (θ = 3.4 & 16º). Significant scale effects were observed in terms of distributions of bubble count rates, turbulence intensity and bubble/droplet chord sizes. Basically the number of entrained bubble sizes and turbulence levels were drastically underestimated with the smallest step sizes. Further it is demonstrated that the selection of the basic criterion to define scale effects is critical : e.g., flow resistance, air concentration distributions, or turbulence levels.

It is believed that the new results are the first systematic study of scale effects in air-water flows at microscopic scales. The results emphasise that physical modelling of stepped chutes is more sensitive to scale effects than classical smooth-invert chute studies, and this is consistent with basic dimensional analysis. While the findings

were obtained for two moderate slopes (θ = 3.4 & 16º), it is thought that the outcomes are valid for a wider range of chute geometry and flow conditions.

6. ACKNOWLEDGMENTS

The writers acknowledge the assistance of Mr Graham Illidge and Dr L. Toombes. The first writer acknowledges the financial support of the National Council for Science and Technology of Mexico (CONACYT). The second author acknowledges the assistance of his students L. Rowlands, M. Condon, M. Eastman and N. Van Schagen.

7. REFERENCES

BaCaRa (1991). "Etude de la Dissipation d'Energie sur les Evacuateurs à Marches." ('Study of the Energy Dissipation on Stepped Spillways.') *Rapport d'Essais*, Projet National BaCaRa, CEMAGREF-SCP, Aix-en-Provence, France, Oct., 111 pages (in French).

Boes, R.M. (2000). "Zweiphasenstroömung und Energieumsetzung an Grosskaskaden." ('Two-Phase Flow and Energy Dissipation on Cascades.') *Ph.D. thesis*, VAW-ETH, Zürich, Switzerland (in German). (also *Mitteilungen der Versuchsanstalt fur Wasserbau, Hydrologie und Glaziologie*, ETH-Zurich, Switzerland, No. 166).

Chanson, H. (2001). "The Hydraulics of Stepped Chutes and Spillways." *Balkema*, Lisse, The Netherlands, 418 pages. {http://www.uq.edu.au/~e2hchans/reprints/book4.htm}

Chanson, H. (2002). "Air-Water Flow Measurements with Intrusive Phase-Detection Probes. Can we Improve their Interpretation ?." *Jl of Hyd. Engrg.*, ASCE, Vol. 128, No. 3, pp. 252-255.

Chanson, H. (2004). "The Hydraulics of Open Channel Flows : An Introduction." *Butterworth-Heinemann*, Oxford, UK, 2nd edition. {http://www.uq.edu.au/~e2hchans/reprints/book3_2.htm}

Chanson, H., and Toombes, L. (2002). "Air-Water Flows down Stepped chutes : Turbulence and Flow Structure Observations." *Intl Jl of Multiphase Flow*, Vol. 27, No. 11, pp. 1737-1761.

Chanson, H., Yasuda, Y., and Ohtsu, I. (2002). "Flow Resistance in Skimming Flows and its Modelling." *Can Jl of Civ. Eng.*, Vol. 29, No. 6, pp. 809-819.

Djenidi, L., Elavarasan, R., and Antonia, R.A. (1999). "The Turbulent Boundary Layer over Transverse Square Cavities." *Jl Fluid Mech.*, Vol. 395, pp. 271-294.

Henderson, F.M. (1966). "Open Channel Flow." *MacMillan Company*, New York, USA.

Knight, D.W., and Macdonald, J.A. (1979). "Hydraulic Resistance of Artificial Strip Roughness." *Jl of Hyd. Div.*, ASCE, Vol. 105, No. HY6, June, pp. 675-690.

Ohtsu, I., and Yasuda, Y. (1998). "Hydraulic Characteristics of Stepped Channel Flows." *Workshop on Flow Characteristics around Hydraulic Structures and River Environment*, University Research Center, Nihon University, Tokyo, Japan, November, Edited by I. Ohtsu and Y. Yasuda, 55 pages.